

编号: 2024-0170

## 检索报告

受南通市第一人民医院王蕾的委托,对其所提交的学术论文被收录和引用情况在 Web of Science(Science Citation Index Expanded)中进行了检索,以下 1 篇论文被 SCIE 收录。

### 第 1 条,共 1 条

**标题: Molecular Investigation and Preliminary Validation of Candidate Genes Associated with Neurological Damage in Heat Stroke**

作者: Wang, L (Wang, Lei); Shen, YM (Shen, Yi-ming); Chu, X (Chu, Xin); Peng, Q (Peng, Qiang); Cao, ZY (Cao, Zhi-yong); Cao, H (Cao, Hui); Jia, HY (Jia, Han-yu); Zhu, BF (Zhu, Bao-feng); Zhang, Y (Zhang, Yi)

来源出版物: MOLECULAR NEUROBIOLOGY DOI: 10.1007/s12035-024-03968-1 提前访问日期: JAN 2024

Web of Science 核心合集中的 "被引频次": 0

入藏号: WOS:001152762200002

文献类型: Article; Early Access

地址: [Wang, Lei; Shen, Yi-ming; Chu, Xin; Peng, Qiang; Zhu, Bao-feng] Nantong Univ, Dept Emergency Ctr, Affiliated Hosp 2, 6 North Child Lane Rd, Nantong, Peoples R China.

[Cao, Zhi-yong] Nantong Univ, Dept Neurol, Affiliated Hosp 2, 6 North Child Lane Rd, Nantong, Peoples R China.

[Cao, Hui] Nantong Univ, Affiliated Hosp 2, Dept Rehabil, 6 North Child Lane Rd, Nantong, Peoples R China.

[Jia, Han-yu; Zhang, Yi] Nantong Univ, Affiliated Hosp 2, Res & Educ Sect, 6 North Child Lane Rd, Nantong, Peoples R China.

[Zhang, Yi] Nantong Univ, Dept Neurosurg, Affiliated Hosp 2, 6 North Child Lane Rd, Nantong, Peoples R China.

通讯作者地址: Zhu, BF (通讯作者), Nantong Univ, Dept Emergency Ctr, Affiliated Hosp 2, 6 North Child Lane Rd, Nantong, Peoples R China.

Zhang, Y (通讯作者), Nantong Univ, Affiliated Hosp 2, Res & Educ Sect, 6 North Child Lane Rd, Nantong, Peoples R China.

Zhang, Y (通讯作者), Nantong Univ, Dept Neurosurg, Affiliated Hosp 2, 6 North Child Lane Rd, Nantong, Peoples R China.

电子邮件地址: bfzhunt1@163.com; zhangyi9285@126.com

ISSN: 0893-7648

eISSN: 1559-1182

期刊影响因子 (2022): 5.1

中科院 2023 年期刊大类分区 (升级版): 2 区

特此证明!





# Molecular Investigation and Preliminary Validation of Candidate Genes Associated with Neurological Damage in Heat Stroke

Lei Wang<sup>1</sup> · Yi-ming Shen<sup>1</sup> · Xin Chu<sup>1</sup> · Qiang Peng<sup>1</sup> · Zhi-yong Cao<sup>2</sup> · Hui Cao<sup>3</sup> · Han-yu Jia<sup>4</sup> · Bao-feng Zhu<sup>1</sup> · Yi Zhang<sup>4,5</sup>

Received: 6 September 2023 / Accepted: 16 January 2024  
© The Author(s), under exclusive licence to Springer Science+Business Media, LLC, part of Springer Nature 2024

## Abstract

Heat stroke (HS) is a severe medical condition characterized by a systemic inflammatory response that may precipitate multi-organ dysfunction, with a particular predilection for inducing profound central nervous system impairments. We aim to employ bioinformatics techniques for the retrieval and analysis of genes associated with heat stroke-induced neurological damage. We performed a comprehensive analysis of the GSE64778 dataset from the Sequence Read Archive, resulting in the identification of 1178 significantly differentially expressed genes (DEGs). We retrieved 2914 genes associated with heat stroke from the GeneCards database and 2377 genes associated with heat stroke from the Comparative Toxicogenomics Database (CTD). The intersection of the top 300 DEGs in the GSE64778 dataset intersected with the search results of GeneCards and CTD, yielding 25 final candidates for DEGs associated with heat stroke. Gene Ontology functional annotation results indicated that the target genes were mainly involved in apoptosis, stress response, and negative regulation of cellular processes and function in processes such as protein dimerization and protein binding. The Kyoto Encyclopedia of Genes and Genomes pathway enrichment analysis revealed a predominant enrichment of candidate target genes within the PI3K-AKT signaling pathway. Subsequent protein–protein interaction network analysis highlighted HSP90aa1 as a central gene, indicating its pivotal role by possessing the highest number of edges among the genes enriched in the PI3K-AKT signaling pathway. Quantitative reverse transcription-polymerase chain reaction analysis performed on blood samples from patients validated the expression of Hsp90aa1 in individuals exhibiting early neurological damage in HS, consistent with the findings from the mRNA bioinformatics analysis. Additionally, the bioinformatics analysis of the upstream microRNAs (miRNAs) regulating HSP90aa1 and the target miRNAs associated with candidate long non-coding RNAs (lncRNAs) identified three lncRNAs, eight miRNAs, and one mRNA in the regulatory network. The DIANA Tools database and algorithms were employed for pathway enrichment and correlation analysis, revealing a significant association between LOC102547734 and MIR-206-3p, with the latter being identified as a target binding site. Moreover, the analysis unveiled a correlation between MIR-206-3p and HSP90aa1, implicating the latter as a potential target binding site within the regulatory network.

**Keywords** Bioinformatics · ceRNA network · Heat stroke · Hsp90aa1 · LOC102547734 · miR-206-3p · Nerve damage · PI3K-AKT signal pathway

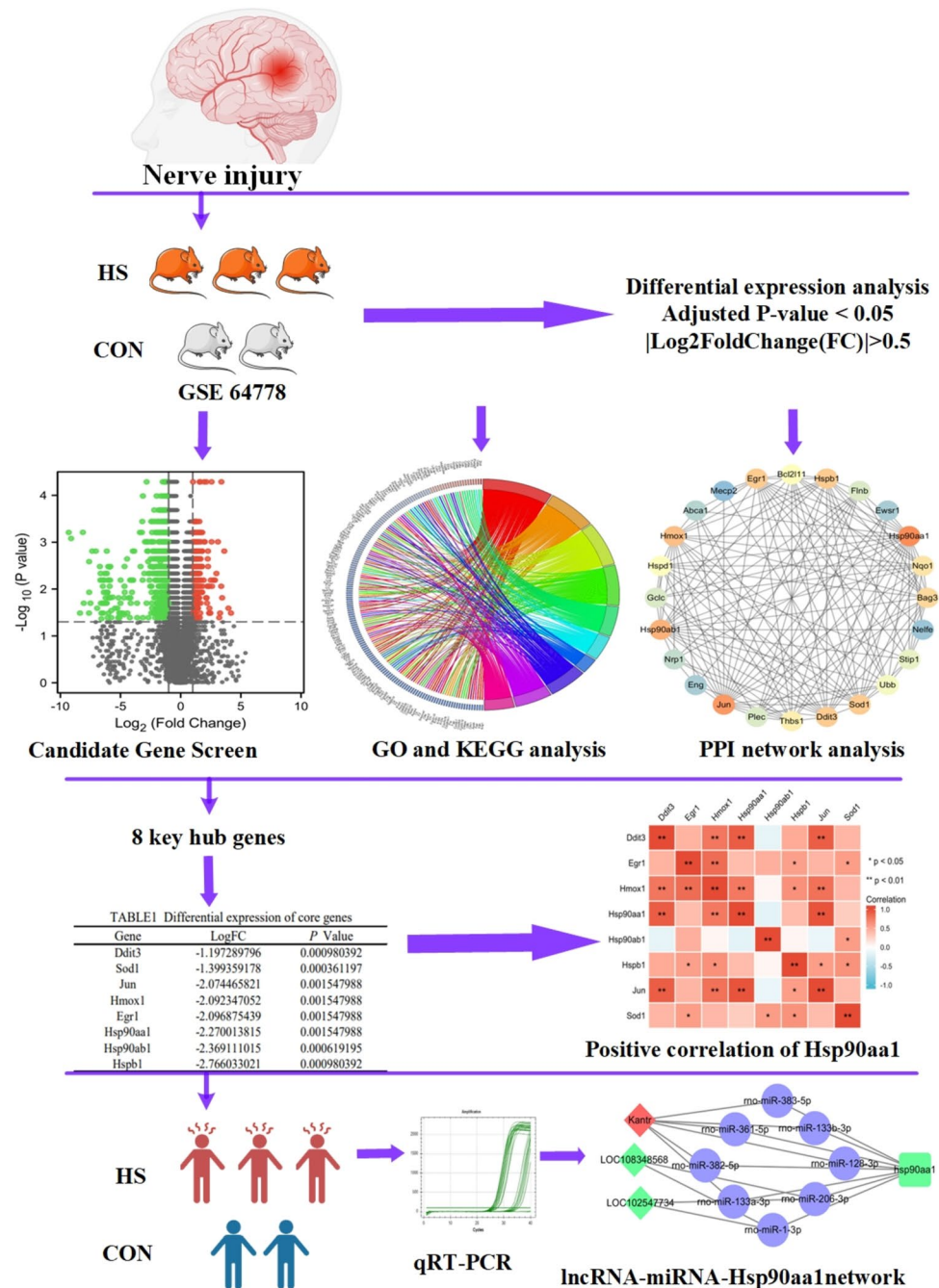
**Novelty and Impact** Hsp90aa1 can serve as a prognostic marker for heat stroke (HS). The PI3K-AKT signaling pathway may be involved in the regulation of neurological damage in HS. The LOC102547734-miR-206-3p-Hsp90aa1 regulatory network may inhibit the development of neurological damage in HS. LOC102547734-MIR-206-3p-HSP90aa1 might be a key ceRNA network that prevents HS nerve damage.

Extended author information available on the last page of the article

## Introduction

Heat stroke (HS) is a clinical syndrome characterized by a rapid increase in the core body temperature ( $> 40^{\circ}\text{C}$ ) caused by an imbalance between heat production and heat dissipation, which in turn leads to a systemic inflammatory response and multi-organ dysfunction, especially severe central nervous system damage. Incomplete epidemiological data shows a mortality rate of over 60% [1, 2]. Currently,

**Fig. 1** Design idea of this study. GSE60436 dataset downloaded from the GEO database, combining GeneCards and the CTD database to screen candidate target genes. The R software was used to process the data, including quality control, normalization, and background correction. A total of 25 differentially expressed DEGs in the dataset were identified by difference analysis, and GO and KEGG enrichment analyses were performed. At the same time, 8 hub genes were identified by PPI analysis and then verified with qRT-PCR. Finally, the ceRNA regulatory network was screened and constructed using the RNAInter, miRWalk, RAID2, and miRDB databases



there are inconsistent reports on regional epidemiological data in the country. Upon reviewing the case data from July 30, 2015, to October 5, 2020, the mortality rate was 12.86%, considering its correlation with a single-center sample. Patients with severe heat stroke and consciousness disorders may sometimes have concurrent traumatic brain injury or aspiration, making clinical manifestations and diagnosis more complex. Accurately seeking biomarkers to predict the occurrence and development patterns of severe heat stroke will facilitate rapid identification and treatment. Therefore, this study continues to delve into the molecular

mechanisms. Cranial MRI reveals midbrain damage that manifests itself as cerebral edema, hemorrhage, or infarction. Cerebral edema mainly presents as vasogenic edema owing to increased capillary permeability and cytotoxic edema resulting from cell membrane dysfunction [3]. Cytotoxic edema is highly likely to lead to serious sequelae and has become a public health emergency of widespread concern in recent years [4]. The pathogenesis of HS involves a complex interaction of multiple cellular processes [5], notably encompassing inflammation, oxidative stress, endoplasmic reticulum stress, and mitochondrial dysfunction.

**Table 1** PCR primer sequences

Gene name	Forward primer(5'–3')	Reverse primer (5'–3')
Hsp90aa1	GAAGGAATTTGAGGGGAAGACTTTA	TGCCATGTAACCCATTGTTGAG
GAPDH	GGAAGCTTGTCATCAATGGAAATC	TGATGACCCTTTTGGCTCCC

The human Hsp90 (heat shock protein 90, Hsp90) family includes Hsp90 $\alpha$  and Hsp90 $\beta$  in the cytoplasm, glucose-regulated protein 94 (Grp94) in the endoplasmic reticulum, and tumor necrosis factor receptor-associated protein 1 (Trap1) in the mitochondria. The amino acid sequences of Hsp90 $\alpha$  and Hsp90 $\beta$  are highly homologous; however, they are expressed in different ways, with Hsp90 $\alpha$  being induced by stress, whereas Hsp90 $\beta$  is constitutively expressed to support normal cell function [6]. Hsp90 is essential for the activity of many signaling molecules and transcription factors involved in cellular inflammation, inducing a variety of pro-inflammatory cytokines, and effectively enhancing the extracellular

immune system [7] in cancer, viral infections, inflammatory diseases, and neurodegenerative diseases [8–10].

Hsp90 plays an important role in protecting neuronal proteins, which tend to accumulate abnormally and form toxic aggregates. Hsp90 inhibits protein aggregation associated with neurodegenerative diseases such as Alzheimer's disease (AD) and Parkinson's disease (PD) [11], and activation of Hsp90 expression improves cognitive deficits in AD mouse models [12]. In contrast, Hsp70 and Hsp90 are involved in multi-organ dysfunction and inflammatory responses in rat pyrexia. However, the upregulation of these genes is associated with the restoration of proteostasis [13].

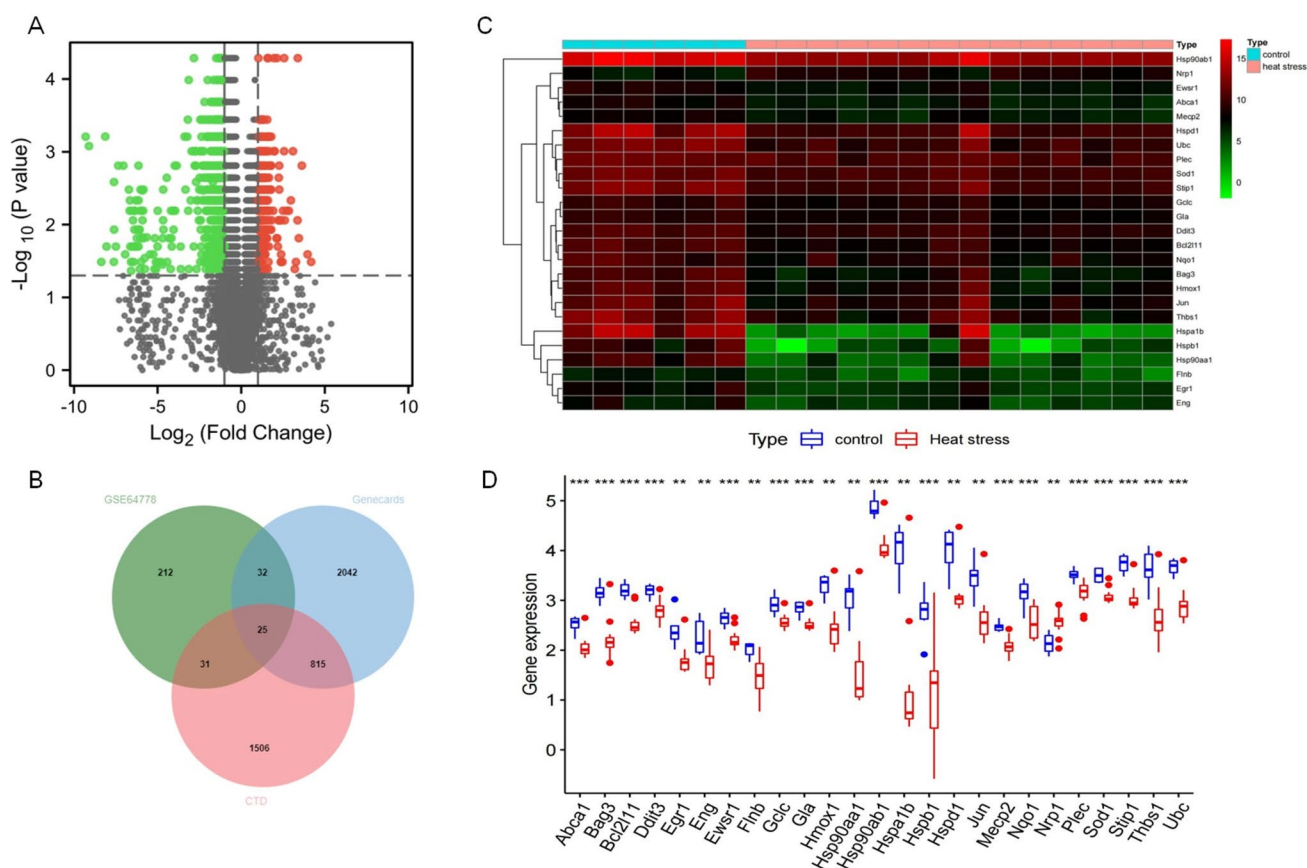


**Fig. 2** Screening of candidate genes related to the occurrence of HS. **A** Volcano plot of differential gene expression in the HS-related dataset GSE64778 from the public database; red dots indicate high-expression genes; green dots indicate low-expression genes, and gray dots indicate no significant difference; the horizontal axis indicates the logarithmic value of the multiple of difference (FC) between different subgroups with 2 as the bottom, i.e.,  $\log_2$  (fold change); the vertical axis represents the negative 10 of the  $P$ -value of the dif-

ference significance test as the bottom logarithm, i.e.,  $-\log_{10}$  ( $P$ -value); **B** Venn diagram of the intersection of the top 300 DEGs in dataset GSE64778 with the GeneCards and CTD database of HS-related genes; **C** heat map of the 25 candidate DEGs expressed in the GSE64778 dataset; **D** heat map of the 25 candidate DEGs in the GSE64778 dataset with differential expression box line plots,  $^{**}P < 0.01$  compared with the control group;  $^{***}P < 0.001$  compared with the control group. Control group,  $n = 6$ ; heat stroke group,  $n = 14$



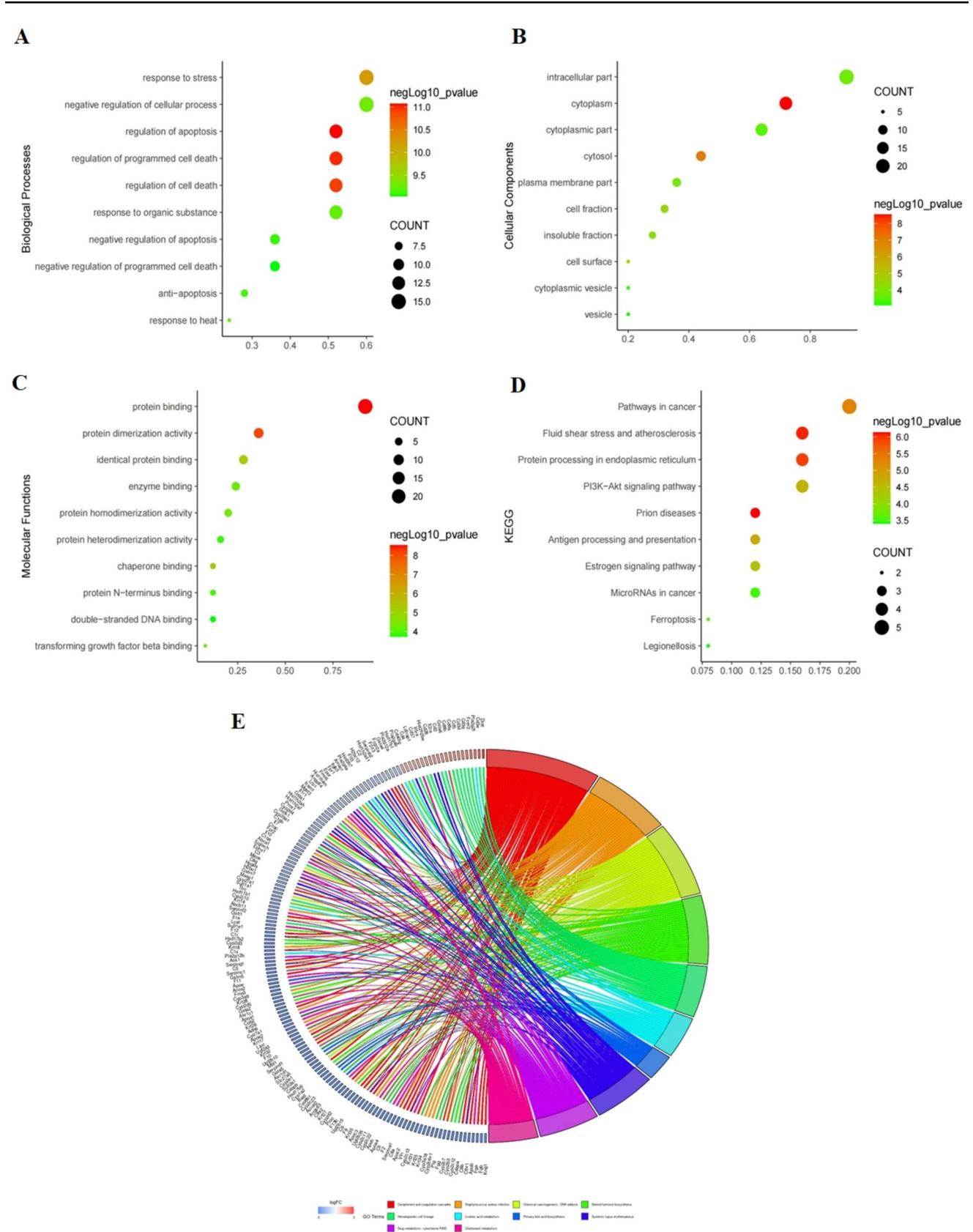


**Fig. 3** Functional enrichment analysis of candidate genes related to the occurrence of HS. **A** GO functional analysis of DEGs in BP; **B** GO functional analysis at CC level; **C** GO functional analysis at MF level; **D** KEGG pathway enrichment analysis. The horizontal coordinates represent gene ratio; different colors represent  $-\log_{10} P$ -value; the larger the value, the darker the color, indicating that the smaller the  $P$ -value, the more significant the difference; the circle size indicates the amount of gene enrichment; the larger the circle, the greater the number of gene enrichments. **E** Chordal graph of enriched GO terms

In our previous work, we confirmed the early activation of microglial polarization in the brain tissue of heat stroke patients and the involvement of neuroinflammatory responses in brain tissue damage caused by heat stroke. This study will continue to delve into the molecular mechanisms. Bowyer et al. conducted a study to analyze hyperthermia-induced alterations in immune-related genes using blood samples. They generated the gene microarray dataset GSE64778 [14], which was deposited in the Gene Expression Omnibus (GEO) database of the National Center for Biotechnology Information. We screened the GSE64778 dataset to identify the key factors associated with the pathogenesis of central nervous system damage in HS. We used correlation analysis, Gene Ontology (GO) enrichment analysis, the Kyoto Encyclopedia of Genes and Genomes (KEGG) pathway analysis, and protein–protein interaction (PPI) network analysis of target differentially expressed genes (DEGs) and verified them in clinical samples using quantitative real-time polymerase chain reaction (qRT-PCR). Finally, we used intersectional bioinformatics analysis of the verified target gene set and online databases to predict the lncRNA-miRNA-mRNA co-expression network (competing endogenous RNAs, ceRNA). Our results provide a platform to elucidate the molecular and cellular mechanisms of neurological damage in HS and to identify potential diagnostic and therapeutic targets (Fig. 1).

## Materials and Methods

### Sample and Study Respondents

This study was approved by the Second Hospital of Nantong University, Jiangsu Province, China (approval number: 2021KT007), and complied with the Declaration of Helsinki. We selected patients who were diagnosed with HS between June 1 and August 30, 2022, based on the International Classification of Diseases ([ninth revision], Clinical Modification [ICD-9-CM] codes, HS, ICD-9-CM 992.0), accompanied by manifestations of central nervous system dysfunction (e.g., coma, convulsions, delirium, and abnormal behavior) [15], and admitted for less than 24 h of illness. We included patients willing to provide signed consent to

collect peripheral blood for medical studies. The exclusion criterion was the presence of oncological, hematological, or immune-related underlying diseases. Fourteen patients with HS were enrolled in the study.

For the HS prognosis, they were divided into a survival group ( $n = 10$ ) and a death group ( $n = 4$ ), with a male-to-female ratio of 8:6, age of 54–73 years, and a mean of  $67 \pm 6.81$  years. The time of onset was 3–11 h, with a mean of  $6.89 \pm 2.74$  h. Serum was collected from patients at the time of presentation. Additional data were collected from the four patients in the death group, including survival time from onset to death of 32–56 h and a mean of  $38.13 \pm 12.3$  h. Serum samples were collected from these four patients at 24 h of onset and subsequently stored in a refrigerator at  $-20^\circ\text{C}$ .

### GEO Database Transcriptome Sequencing Data Acquisition

We retrieved data sets from the GEO database (<https://www.ncbi.nlm.nih.gov/gds>) using “Heat Stroke”, “Neurotoxic”, and “Circulating Whole Blood” as the keywords; the species was limited to “*Rattus norvegicus*”, and we selected “Expression profiling by high throughput sequencing” as the experiment type. The GSE64778 dataset (annotation platform GPL14844) included whole blood transcriptome data from 14 rats with neurotoxicity caused by a high thermal environment ( $39^\circ\text{C}$ ) and six normal rats as controls. We selected the 20 samples from this dataset as our study subjects.

### Quality Control and Reference Genome Comparison

The RNA sequencing raw data for the study subjects were directly retrieved from the Sequence Read Archive (SRA) at <https://www.ncbi.nlm.nih.gov/sra/docs/> and subsequently converted to the FASTQ format within the Linux operating system. To assess data quality comprehensively, including average quality, GC content proportion, presence of N bases, and repetitive sequence length, the FastQC software (v0.11.8, [www.bioinformatics.babraham.ac.uk](http://www.bioinformatics.babraham.ac.uk)) was employed. The Cutadapt software (v1.18, [www.bioinformatics.babraham.ac.uk](http://www.bioinformatics.babraham.ac.uk)) was used to eliminate the joint FASTQ data sequences and reads with an N content exceeding 5%. The pertinent parameters were configured to permit mismatch and insertion losses, as well as partial matches. Subsequently, the top 70% of high-quality reads with a base mass above 20 were extracted using the FASTX Toolkit software (v0.0.13, [http://hannonlab.cshl.edu/fastx\\_toolkit/](http://hannonlab.cshl.edu/fastx_toolkit/)). The double-ended sequences were then repaired using BBMap software (<https://sourceforge.net/projects/bbmap/>). Finally, the filtered fragments of high-quality reads were compared with the rat reference genome utilizing hisat2 software (0.7.12).

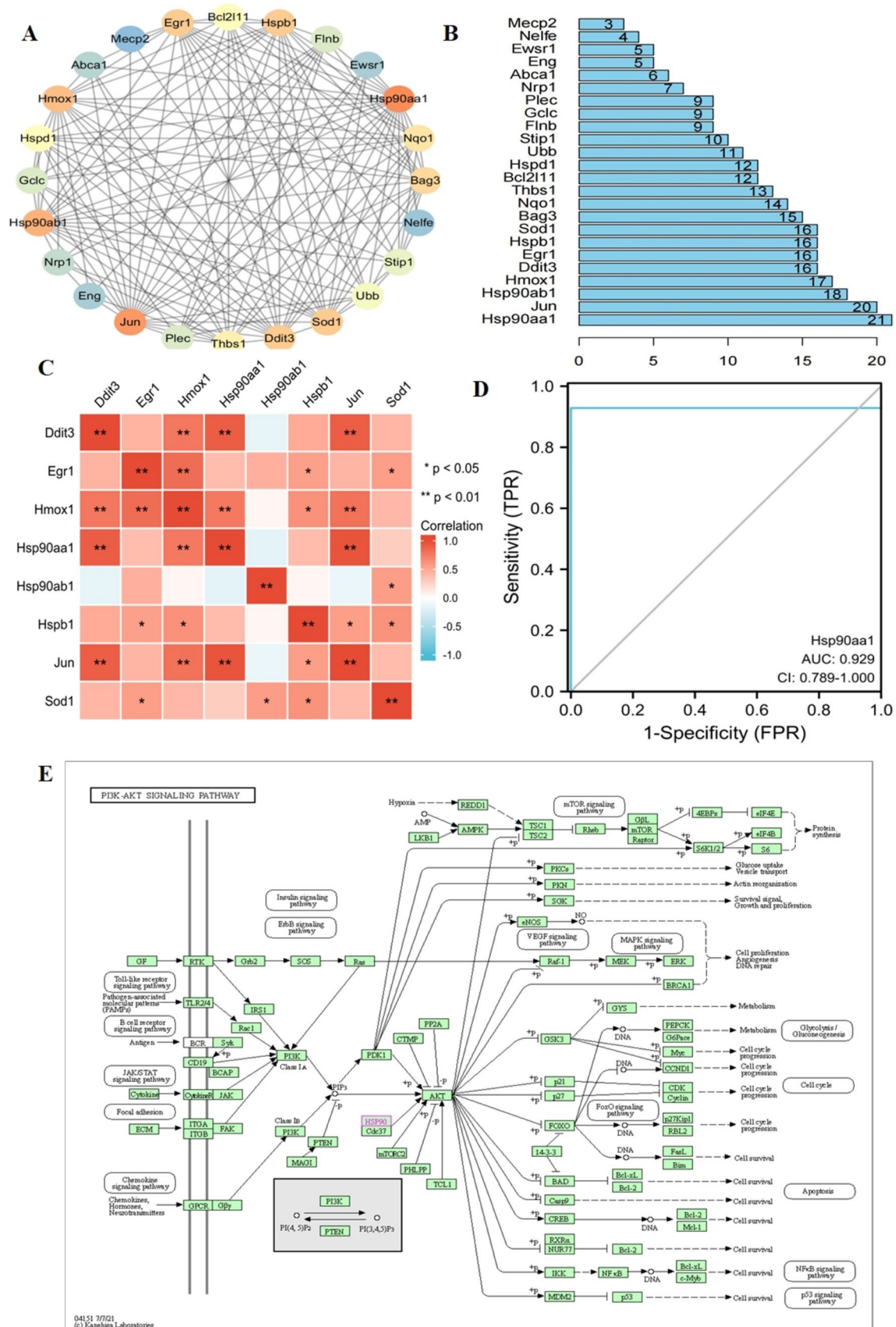




**Fig. 4** Hsp90aa1 is involved in regulating neurological damage in HS. **A** Cytoscape software was used to plot the PPI network of 25 candidate DEGs—nodes indicate proteins and edges indicate protein interconnections; **B** bar graph of 25 candidate DEGs sorted by degree; **C** analysis of the correlation of expression of 25 candidate DEGs in the heat stroke group using dataset GSE64778, squares in the graph. The color of the square indicates the strength of the correlation between genes, with red indicating a stronger positive correlation, blue indicating a stronger negative correlation, and asterisk (\*) indicating the significance of the correlation; **D** ROC curves for analyzing the accuracy of Hsp90aa1 in predicting the occurrence of HS, with the false positive rate (FPR) as the horizontal coordinate and the true positive rate (TPR) as the vertical coordinate. **E** KEGG pathway analysis of the specific regulatory relationship of Hsp90aa1 in the PI3K-AKT signaling pathway

## Analysis of Differential Gene Expression

Read count analysis for both long non-coding RNAs (lncRNAs) and messenger RNAs (mRNAs) was carried out using the R language “edgeR” package, accessible at <http://www.bioconductor.org/packages/release/bioc/html/edgeR.html>. Differential expression analysis was subsequently conducted separately for lncRNAs and mRNAs, with the criteria for differential gene screening set as  $|\log\text{FC}| > 1$  and a  $P$ -value of  $< 0.05$ . The R package “ggplot2” was used to plot volcano plots and differentially expressed gene box plots, and the R package “heatmap” was used to plot the differential gene expression heat maps. Correlation analysis of the mRNA expression of the candidate genes was performed using the R “corrplot” package.

## Disease-Related Database Search

Heat stroke-related target genes were selected from the Gene Cards database (<https://www.genecards.org/>) and Comparative Toxicogenomics databases (CTD) (<http://ctdbase.org/>). Specifically, target genes with a relevance score  $\geq 1$  from GeneCards and an inference score  $\geq 1$  from CTD were designated as disease-related target genes. Given that the genes obtained from the database were initially human disease-related genes, the “homologene” R package was used for the homologous transformation of these human disease target genes and rat genes, resulting in the identification of rat heat stroke-related target genes.

## Functional Enrichment Analysis of Candidate Genes and Protein Interaction Network Construction

Candidate genes were identified using the Venn tool (<http://jvenn.toulouse.inra.fr/app/example.html>.) This involved determining the intersection of genes associated with heat shock-induced neurotoxicity and those identified as disease-associated target genes within the GSE64778 dataset. To gain a deeper understanding of the biological

implications of these candidate genes in the onset and progression of neurotoxicity resulting from heat shock, as well as to elucidate their potential molecular regulatory relationships, we conducted GO and KEGG analyses of the differential genes. The imported genes were subjected to Network Ontology Analysis (<http://app.aporc.org/NOA/>) and the KOBAS databases (<http://kobas.cbi.pku.edu.cn/>) for GO function and KEGG pathway enrichment analyses. The outcomes were visualized using the Image GP website (<http://www.ehbio.com/ImageGP/index.php/Home/Index/index.html>). The enrichment results, covering Biological Processes (BP), Cellular Components (CC), and Molecular Functions (MF), were mapped. A significance threshold of  $P < 0.05$  was considered to indicate statistical significance in the enrichment analyses.

The candidate genes were imported into the STRING database ([https://cn.string-db.org/cgi/input?sessionId=b92G0n5gdTKt&input\\_page\\_show\\_search=off](https://cn.string-db.org/cgi/input?sessionId=b92G0n5gdTKt&input_page_show_search=off)) to acquire information on protein–protein interactions (PPI). A PPI network was constructed, specifically limiting the species to “Rattus norvegicus.” Subsequently, the regulatory relationship network was imported into the Cytoscape software (v3.6.0) for association and visualization analysis. In the visualization, the degree and magnitude of the combined score value are represented by color, and the candidate genes are ranked based on their degree values.

## ROC Curve Analysis

Receiver operating characteristic (ROC) curve analysis was conducted and graphically represented using the R language pROC package, which can be accessed at <https://cran.r-project.org/web/packages/pROC/index.html>, in conjunction with the ggplot2 package. The area under the ROC curve (AUC) was calculated to assess the predictive performance of this factor. A factor was deemed to have good predictive performance when the AUC was greater than 0.5, and the associated  $P$ -value was less than 0.05.

## Prediction of Upstream microRNAs and lncRNAs of Candidate Genes

To predict upstream microRNAs (miRNAs) targeting candidate target genes (mRNAs), we used the miR-Walk (<http://mirwalk.umm.uni-heidelberg.de/>), RAID v2.0 (<http://www.rna-society.org/raid2/index.html>), and RNAInter (<http://rnainter.org/>) databases. The obtained results were further processed by taking intersections using the Jvenn tool. Subsequently, miRNAs targeting the candidate lncRNAs were predicted using the miRDB database (<http://mirdb.org/index.html>). Following this, an lncRNA-miRNA-mRNA co-expression regulatory network was constructed, and a visual representation



of the network was generated using Cytoscape software (v3.6.0). Furthermore, pathways enriched by candidate miRNA target genes were analyzed with the mirPath v.3 tool available at <http://diana.imis.athena-innovation.gr/DianaTools/index.php?r=mirpath/index> in the DIANA TOOLS database.

### Quantitative RT-PCR

cDNA was reverse-transcribed from total RNA using the UEIris II RT-PCR System (Suzhou Yuheng Biological Co., Ltd.) in strict accordance with the manufacturer's instructions, and qRT-PCR was performed using 2×SYBR Green qPCR Master Mix (Suzhou Yuheng Biological Co., Ltd.). The RT-qPCR primer sequences are listed in Table 1. Gene expression was determined using the  $2^{-\Delta\Delta C_t}$  method. Glyceraldehyde 3-phosphate dehydrogenase (GAPDH) was used as the internal control.

### Western Blot

The cultured cells were lysed with radioimmunoprecipitation assay (RIPA) lysis buffer (Servicebio, Wuhan, China) containing protease and phosphatase inhibitors, and protein concentrations were determined using a bicinchoninic acid assay (BCA) kit (Servicebio, Wuhan, China). Samples were separated using 10% sodium dodecyl sulfate–polyacrylamide gel electrophoresis (SDS-PAGE) at 120 V and transferred to polyvinylidene membranes. The membranes were then closed in a 5% protein reduction loading buffer for 1 h. The membranes were incubated with primary antibodies against Hsp90 (Servicebio, Wuhan, China) and GAPDH (Servicebio, Wuhan, China) at 4 °C overnight. After washing with Tris-buffered saline-Tween (TBST) for 15 min, the membranes were incubated with HRP-goat anti-mouse secondary antibodies (Servicebio, Wuhan, China) for 1 h at room temperature. Following this procedure, the membranes were washed with Tris-buffered saline with Tween 20 (TBST) for 45 min. Visualization was performed using an enhanced chemiluminescence kit. The collected images were examined using the ImageJ software (version 6.0; Media Cybernetics, Inc.).

### Statistical Analysis

Each in vitro experiment was repeated at least thrice. Statistical analyses were performed using GraphPad Prism software (version 8.0). Based on the homogeneity of the variance test, Student's *t*-test was performed, and  $P < 0.05$ .

## Results

### Screening of Key Genes for Neurological Damage in HS

The mRNA differential analysis conducted on the SRA data from GSE64778 identified 1178 DEGs. Among these, 322 genes were upregulated, while 856 genes were downregulated, as illustrated in Fig. 2A. Additionally, a search of the GeneCards database for HS retrieved 2914 genes associated with the condition, and a search of the Comparative Toxicogenomics Database (CTD) for HS yielded 2377 genes. The top 300 DEGs in the GSE64778 dataset (sorted by *P*-value) were intersected with the results of GeneCards and CTD database searches, and 25 candidate DEGs were finally screened (Fig. 2B). Additionally, a heat map (Fig. 2C) and box line plot (Fig. 2D) were drawn. Twenty-four genes were observed, and their expression levels were as follows: *Gla*, *Plec*, *Ddit3*, *Gclc*, *Mecp2*, *Ewsr1*, *Sod1*, *Abca1*, *Flnb*, *Nqo1*, *Eng*, *Bcl2l1*, *Ubc*, *Jun*, *Hmox1*, *Egr1*, *Stip1*, *Hspd1*, *Hspa1b*, *Hsp90aa1*, *Hsp90ab1*, *Bag3*, *Thbs1*, and *Hspb1* were exhibited at low levels, whereas only the *Nrp1* gene was displayed highly expressed.

### GO Function Analysis and KEGG Pathway Enrichment Analysis

Subsequent GO functional annotation and KEGG pathway enrichment analyses of the 25 candidate DEGs revealed significant enrichment. DEGs were predominantly associated with BP, such as regulation of apoptosis (GO:0042981), regulation of programmed cell death (GO:0043067), response to stress (GO:0006950), and negative regulation of cellular processes (GO:0048523). In terms of CC, the main enrichments included the intracellular part (GO:0044424), cytoplasm (GO:0005737), cytoplasmic part (GO:0044444), and cytosol (GO:0005829). MF enrichment included protein binding (GO:0005515), protein dimerization activity (GO:0046983), enzyme binding (GO:0019899), and identity protein binding (GO:0042802) (Fig. 3A–C and E). Functional annotation revealed that the 25 candidate DEGs were mainly enriched in intracellular or cytoplasmic locations; were involved in processes such as apoptosis, stress response, and negative regulation of cellular processes; and exhibited functions related to protein dimerization and protein binding.

KEGG pathway analysis revealed that DEGs were mainly enriched cancer (rno05200), PI3K-AKT signaling (rno04151), fluid shear stress and atherosclerosis (rno05418), and protein processing in the endoplasmic reticulum (rno04141) (Fig. 3D). The enrichment and analysis results strongly suggest that the PI3K/Akt signaling pathway could be a major player in the regulation of central nervous system injury associated with heat stroke.

**Table 2** Results of differential expression of core genes

Gene	LogFC	P-value
Ddit3	-1.197289796	0.000980392
Sod1	-1.399359178	0.000361197
Jun	-2.074465821	0.001547988
Hmox1	-2.092347052	0.001547988
Egr1	-2.096875439	0.001547988
Hsp90aa1	-2.270013815	0.001547988
Hsp90ab1	-2.369111015	0.000619195
Hspb1	-2.766033021	0.000980392

### PPI Analysis of Differentially Expressed Gene-Related Proteins

To identify the core genes associated with neurological damage in HS, we performed PPI analysis on the DEGs obtained from the enrichment analysis. The STRING online database was used to extract protein interaction relationships. Subsequently, the results were imported into the Cytoscape software to construct PPI networks. The resultant PPI network involved 25 nodes and 142 edges, with the color gradient from blue to red representing the degree value. Additionally, the

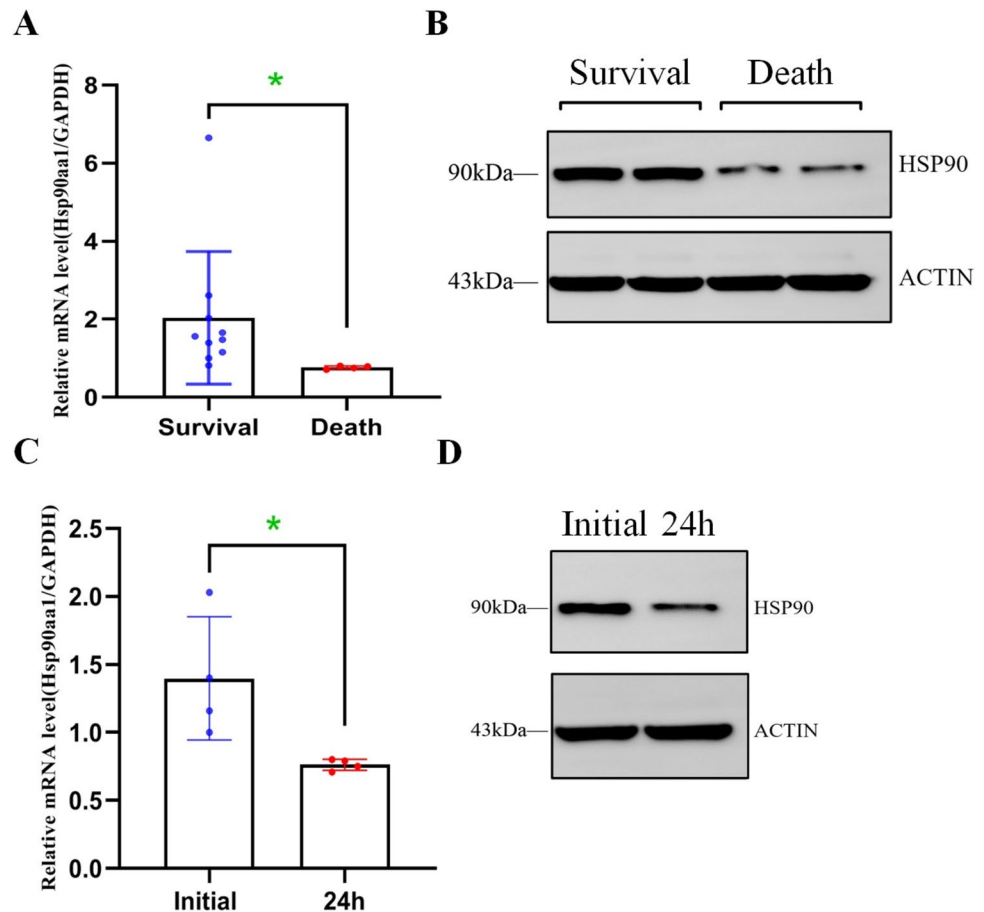
larger the combined score value, the more intense the color, as illustrated in Fig. 4A. The results were ranked according to the degree values, and Hsp90aa1, Jun, Hsp90ab1, Hmox1, Ddit3, Egr1, Hspb1, and Sod1 showed the highest degree values, among which Hsp90aa1 had the highest degree value (Fig. 4B). Correlation analysis of the expression of these eight genes using the expression data from microarray GSE64778 revealed that Hsp90aa1, Jun, Hmox1, and Ddit3 had a stronger positive correlation with other genes (Fig. 4C).

Further analysis of the expression of these eight core genes in microarray GSE64778 revealed that Hsp90aa1, Hsp90ab1, and Hspb1 had a large differential multiplicity (Table 2). In addition, ROC curve analysis showed that the AUC was 0.929, indicating that Hsp90aa1 had high accuracy in predicting the occurrence of HS (Fig. 4D). KEGG pathway analysis revealed a significant role for Hsp90aa1 (Hsp90) in regulating AKT phosphorylation within the PI3K-AKT signaling pathway (rno04151), as illustrated in Fig. 4E.

### Validation of the Hub Genes

To ensure the reliability of the results of the GSE64778 dataset analysis, we used qRT-PCR for validation. The age of the patients in the two groups (survival vs. death group)

**Fig. 5** Expression of Hsp90aa1 in patients with HS. **A** The detection of Hsp90aa1 expression in clinical samples in the survival group vs. death group, which was higher in the survival group than in the death group ( $P < 0.05$ ); **B** Western blot assay in the randomly selected survival group vs. death group; **C** The detection of Hsp90aa1 expression in clinical samples in the initial group vs. the 24-h group, which was higher in the initial group than in the 24-h group ( $P < 0.05$ ); **D** The Western blot assay of the randomly selected initial group vs. 24-h group



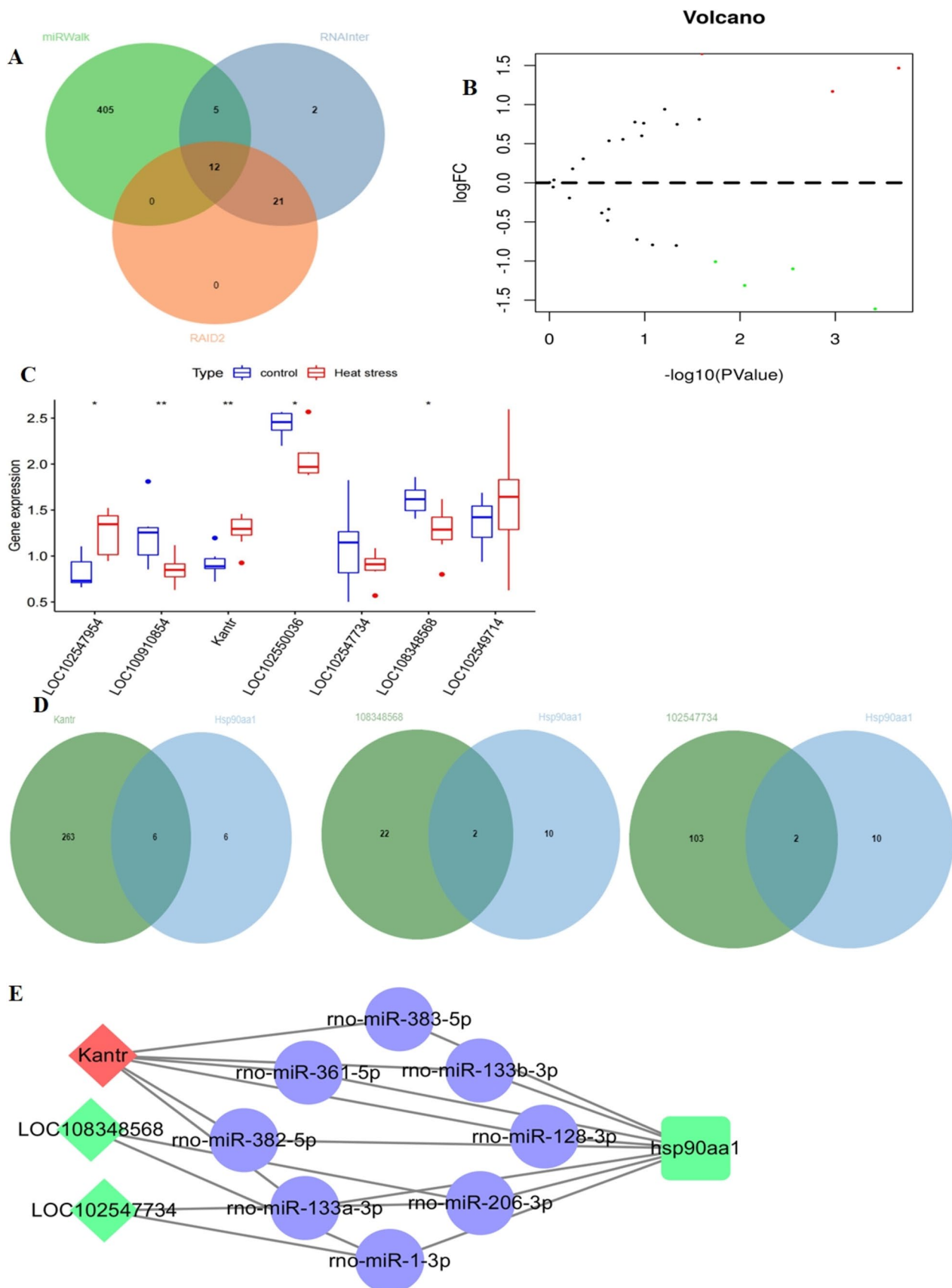


**Fig. 6** Screening of miRNAs and lncRNAs upstream of Hsp90aa1. **A** mirWalk, Venn diagram of the intersection of miRNAs upstream of Hsp90aa1 obtained from RAID2 and RNAInter database predictions; **B** Volcano plot of lncRNA differential expression in the GSE64778 dataset; green dots indicate downregulation; red dots indicate upregulation of expression, and gray dots indicate no significant difference; horizontal axis indicates  $-\log_{10}(P\text{-value})$ , and vertical axis indicates  $\log_2(FC)$ ; **C** Box line plot of significantly differentially expressed lncRNAs in the GSE64778 dataset;  $*P < 0.05$  compared with the control group;  $**P < 0.01$  compared with the control group; control group,  $n = 6$ ; heat stroke group,  $n = 14$ ; **D** Box line plot of targeting candidate lncRNAs and miRNAs of Hsp90aa1 in the intersection Venn diagram; **E** Cytoscape software plotting lncRNA-miRNA-Hsp90aa1 regulatory relationship network; a diamond indicates lncRNA; a circle indicates miRNA, and a square indicates Hsp90aa1

was well-matched, with values of  $(67 \pm 6.75$  vs.  $67 \pm 8.02)$ . Similarly, the time of onset in the two groups (survival vs. death) was closely matched, with values of  $(6.75 \pm 2.86$  vs.  $7.23 \pm 2.81)$ . When total RNA was extracted from the serum samples of 14 patients with HS and compared using qRT-PCR (Fig. 5A), the results indicated that Hsp90aa1 expression was higher in the survival group than in the death group ( $t = 2.369$ ,  $P < 0.05$ ) (Fig. 5B). Moreover, we conducted western blot analysis for expression using serum samples randomly selected from two patients in the survival group and two patients in the death group, and the results were consistent with the PCR findings. Additionally, a further follow-up of four patients in the death group involved collecting sera 24 h after onset. Comparing these samples with sera collected at the beginning of onset, it was observed that Hsp90aa1 expression was higher in the 24-h group than in the initial group ( $t = 4.248$ ,  $P < 0.05$ ) (Fig. 5C). We randomly selected the serum of one patient from the death group for further western blot analysis and observed that Hsp90AA1 expression in the initial group was higher than that in the 24-h group ( $P < 0.05$ ) (Fig. 5D), aligning with the results obtained from PCR analysis.

### Screening of miRNAs and lncRNAs

Currently, there are relatively few studies on miRNAs and lncRNAs in HS. To investigate the mechanism by which lncRNA/miRNA targets Hsp90aa1 to regulate central nervous system damage in HS, we first predicted the upstream miRNAs of Hsp90aa1 using three common online databases (miRWalk, RAID2, and RNAInter). Rat was selected as the species. The search of the miRWalk database yielded 422 miRNAs; the RAID2 database yielded 33 miRNAs, and the RNAInter database yielded 40 miRNAs. The screening results of the above three databases were intersected to obtain 12 miRNAs (rno-miR-128-3p, rno-miR-133a-3p, rno-miR-144-3p, rno-miR-181b-5p, rno-miR-206-3p, rno-miR-383-5p, rno-miR-361-5p, rno-miR-224-5p, rno-miR-1-3p, rno-miR-133b-3p, rno-miR-382-5p, and rno-miR-384-5p) (Fig. 6A).

Differential analysis of lncRNAs was performed on the GSE64778 dataset, yielding seven significantly differentially expressed lncRNAs. Among these, three demonstrated upregulation in expression (LOC102547954, KANTR, and LOC102549714) while four exhibited downregulation (LOC100910854, LOC102550036, LOC102547734, and LOC108348568) (Fig. 6B–C). To predict miRNAs targeting the seven lncRNAs using the miRDB database, an intersection was performed with 12 miRNAs obtained from the previous screening. The analysis revealed that only the miRNAs targeting KANTR, LOC102547734, and LOC108348568 intersected with the miRNAs targeting Hsp90aa1 (Fig. 6D). Subsequently, a network relationship graph of lncRNA-miRNA-mRNA was constructed using the Cytoscape software. The network graph included three lncRNAs, eight miRNAs, and one mRNA (Fig. 6E).

### Key ceRNA Regulatory Network and Signaling Pathway of Nerve Injury in Heat Stroke

Pathway analysis was conducted on the eight target genes of miRNAs within the competing endogenous RNA (ceRNA) network using the mirPath v.3 tool within the DIANA TOOLS database. The results demonstrated that the target genes of rno-miR-133a-3p, rno-miR-133b-3p, and rno-miR-206-3p were significantly enriched in the PI3K-AKT signaling pathway (Fig. 7A). Analysis of the target binding relationship of miRNAs with Hsp90aa1 using the IntaRNA tool within the RNAInter database revealed that rno-miR-361-5p, rno-miR-206-3p, and rno-miR-1-3p had stronger target binding relationships with Hsp90aa1 (Table 3).

The correlations between the expression of Hsp90aa1 and KANTR, LOC102547734, and LOC108348568 were analyzed. The results indicated that KANTR and LOC108348568 were not significantly correlated with Hsp90aa1, whereas LOC102547734 was significant and strongly correlated with Hsp90aa1 (Fig. 7B). Further analysis using miRmap and IntaRNA tools revealed that LOC102547734 possessed target binding sites with miR-206-3p, and miR-206-3p had target binding sites with Hsp90aa1 (Fig. 7C).

### Discussion

Previous studies have shown that the pathogenesis of HS involves a complex interaction between direct cellular damage and the systemic inflammatory response due to heat exposure, ultimately leading to organ damage or multiple organ dysfunction syndrome (MODS) [16]. However, studies on the underlying mechanisms of target organ damage are lacking. Therefore, there is a need to explore new approaches



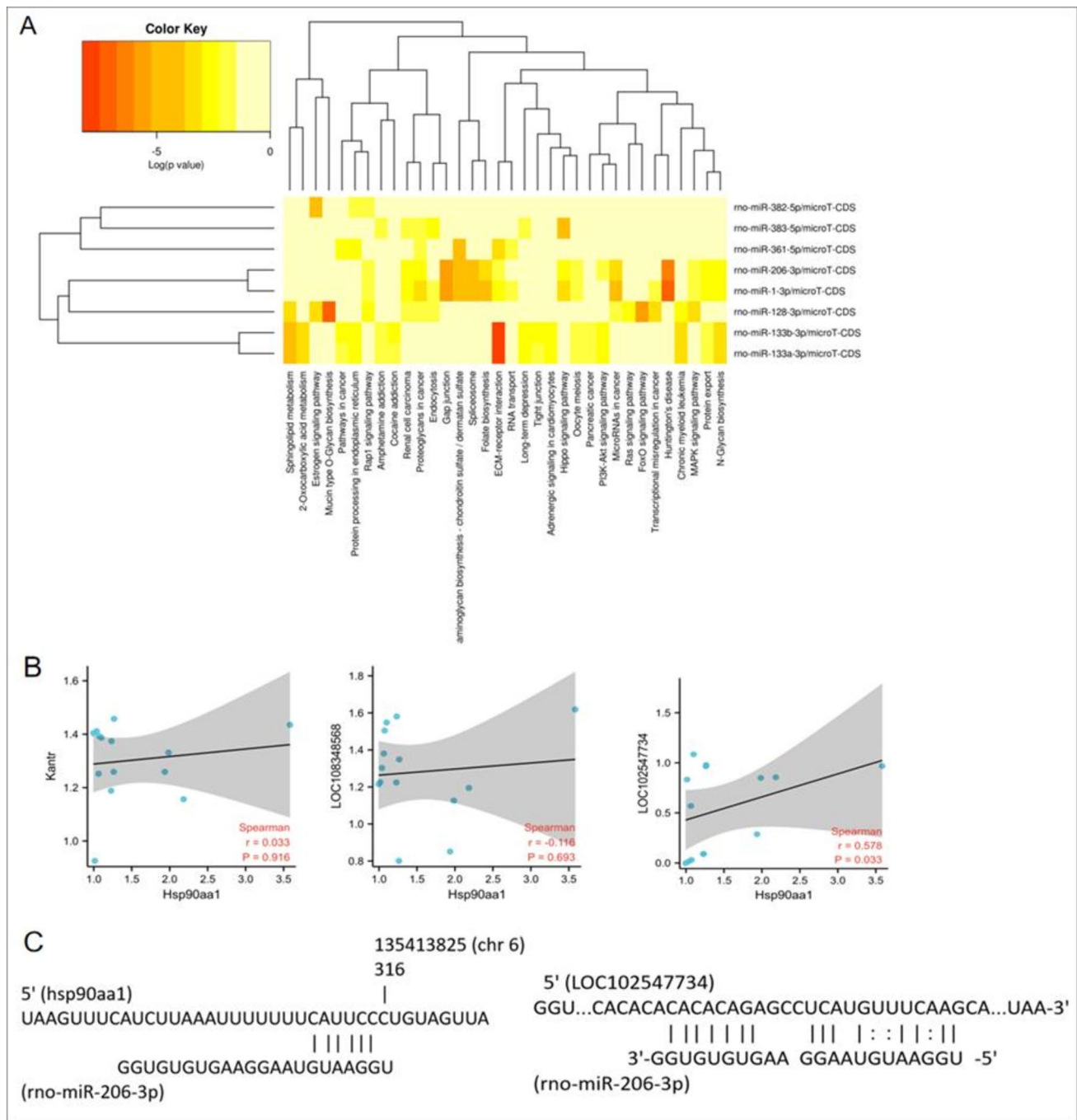


**Fig. 7** A key ceRNA network regulating neurological damage in HS. **A** mirPath v.3 analysis of miRNA target gene enrichment pathway; **B** Spearman analysis of the correlation between Hsp90aa1 and

KANTR, LOC102547734, and LOC108348568 expression; **C** correlation between LOC102547734 and miR-206-3p, miR-206-3p, and target binding sites of Hsp90aa1

to uncover key molecules in the prognosis of HS to screen for possible genes associated with the prognosis of target organ damage.

In this study, a comprehensive analysis of DEGs from GEO data, including GO, KEGG, and PPI analyses, along with GO functional annotation results, revealed that the target genes primarily participated in apoptosis, stress response,

and negative regulation of cellular processes. Additionally, these genes are involved in processes such as protein dimerization and binding. According to the literature, the BDNF-TrkB-PI3K/AKT signaling pathway is suggested to be one of the main pathways involved in the regulation of neurological damage in HS [17, 18]. BDNF, a neurotrophic factor, has been implicated in reducing the infarct size in brain tissue and

mitigating brain injury after the onset of cerebral infarction. BDNF primarily exerts its biological function by binding to and activating the TrkB receptor. The binding of BDNF to TrkB induces receptor dimerization, leading to TrkB phosphorylation, activation of downstream pathways, protection of brain tissue, and promotion of neuronal plasticity [19]. In this context, PI3K serves as a growth factor receptor that is associated with nutritional factors. AKT, a specific protein kinase, is activated in response to growth factors and insulin. Once activated, the PI3K/AKT signaling pathway participates in various cellular processes such as cell growth, proliferation, and nutritional metabolism. As one of the downstream pathways of BDNF/TrkB, the PI3K/AKT signaling pathway plays an important role in the protection of brain tissue and anti-cellular ischemia and hypoxia [20], while the activation of the PI3K/AKT signaling pathway can reduce focal cerebral ischemic neurological damage [21, 22].

Our previous experiments also confirmed the involvement of BDNF in microglial activity during heat-induced nerve damage [23]. In this study, KEGG enrichment analysis suggested that the candidate target genes were mainly enriched in the PI3K/AKT signaling pathway, suggesting that the PI3K/AKT signaling pathway may be involved in regulating neurological damage in HS. Therefore, BDNF, TrkB, and PI3K are closely related to the release of inflammatory factors. Mitochondrial damage, inflammatory responses, oxidative stress, activation of apoptotic factors, and other processes can lead to neurological damage in HS. Liu et al. [24] identified inflammation and oxidative stress-related genes by sequencing in animal models and suggested that immune cells such as macrophages and neutrophils are determinants of prognosis in HS. Inflammation-related genes are the primary genes involved in the development and prognostic regulation of HS. Targeted regulation of the inflammatory response and its signaling pathways may provide a theoretical basis for the study of neurological damage in HS.

Construction of the PPI network revealed that Hsp90aa1, Jun, Hsp90ab1, Hmox1, Ddit3, Egr1, Hspb1, and Sod1 had high degree values; among which, Hsp90aa1 had the highest degree value and may play an important role in the development of neurological damage in HS. Hsp90a is a cytoplasmic chaperone protein that is highly conserved during biological evolution. In recent years, it has become a broad-spectrum tumor marker [25]. Hsp90a is also closely associated with inflammation-related immune processes, inducing a variety of pro-inflammatory cytokines and effectively enhancing the extracellular immune system [26]. The AUC of Hsp90aa1 was 0.929, indicating that Hsp90aa1 was highly accurate in predicting the development of HS. KEGG pathway analysis showed that Hsp90aa1 (Hsp90) regulates AKT phosphorylation, indicating that Hsp90aa1 may mediate the PI3K-AKT signaling pathway to regulate neurological damage in HS. We further validated the selected Hsp90aa1 using qRT-PCR

in sera from 14 patients with heat stroke and nerve damage. Hsp90aa1 was elevated in patients in the survival group compared to the death group, while increased levels of Hsp90aa1 were observed in patients in the death group during the initial phase compared to 24 h later. The changes in the mRNA levels of Hsp90aa1 were consistent with the results of bioinformatics analysis using gene microarray analysis. It is suggested that downregulation of the Hsp90aa1 gene could indicate a poor prognosis for early neurological damage in HS.

In 2011, Pandolfi first proposed the widespread existence of ceRNA molecules (mRNA, lncRNA, pseudogene, etc.) in cells, representing a novel model of gene expression regulation. It integrates multiple ncRNAs (e.g., miRNAs and lncRNAs) and mRNAs into a single regulatory network. They can regulate each other's expression levels through miRNA response elements (MREs) that compete to bind to the same miRNAs [27–29]. It plays an important role in many cellular processes, such as cell differentiation and tissue and organ development. Aberrant expression of exosomal miRNAs and lncRNAs is found in HS-induced vascular endothelial cell damage, and changes in miRNA expression in the circulating exosomes of patients with HS are associated with inflammatory responses [30, 31]. It has also been found that miR-155 promotes a heat stress-induced inflammatory response in microglia [32, 33], suggesting that miRNAs and lncRNAs may play an important role in central nervous system damage in heat stroke; however, there are few studies on miRNAs and lncRNAs related to HS. In this study, to investigate the mechanism by which lncRNA/miRNA targeting Hsp90aa1 regulates central nervous system damage in HS, we predicted the upstream miRNAs of Hsp90aa1 using three common online databases (miRWalk, RAID2, and RNAInter), and the selected species was rat. The network relationship map of lncRNA-miRNA-mRNA was constructed by screening the intersecting genes, and only miRNAs targeting KANTR, LOC102547734, and LOC108348568 were found to intersect with miRNAs targeting Hsp90aa1, and three lncRNAs, eight miRNAs, and one mRNA were included in the constructed lncRNA-miRNA-mRNA network map. The results showed that the

**Table 3** Analysis of miRNAs targeting binding to Hsp90aa1

Target	Position	Query	Position	Energy
Hsp90aa1	2212–2232	rno-miR-361-5p	20–1	–17.2197
Hsp90aa1	1096–1114	rno-miR-206-3p	20–1	–12.6327
Hsp90aa1	285–303	rno-miR-1-3p	21–2	–12.0697
Hsp90aa1	1161–1181	rno-miR-382-5p	21–3	–12.0222
Hsp90aa1	1097–1113	rno-miR-383-5p	20–2	–11.9888
Hsp90aa1	658–680	rno-miR-128-3p	21–1	–11.3213
Hsp90aa1	2511–2535	rno-miR-133a-3p	21–1	–6.54664
Hsp90aa1	2511–2535	rno-miR-133b-3p	21–1	–6.47316

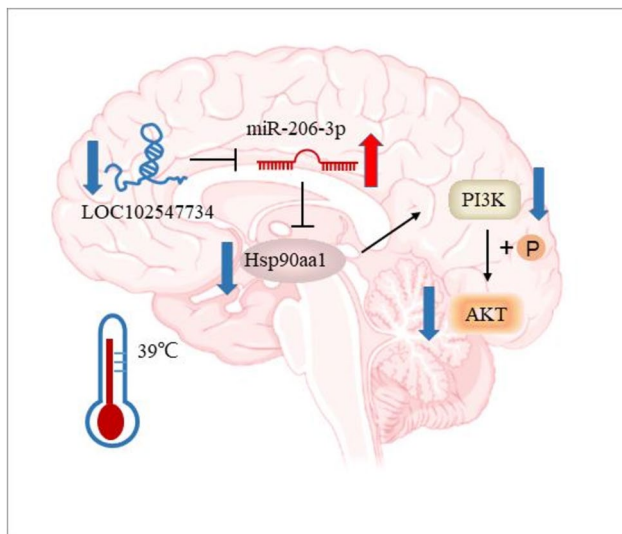


**Fig. 8** Diagram of the mechanistic findings. LOC102547734 has a target binding site with miR-206-3p and miR-206-3p with Hsp90aa1. Red arrows represent up, and blue arrows represent down

target genes of rno-miR-133a-3p, rno-miR-133b-3p, and rno-miR-206-3p were significantly enriched in the PI3K-AKT signaling pathway. Meanwhile, rno-miR-361-5p, rno-miR-206-3p, and rno-miR-1-3p showed a stronger target-binding relationship with Hsp90aa1. Therefore, we hypothesize that rno-miR-206-3p (miR-206-3p) may be involved in heat stroke-associated nerve damage by targeting Hsp90aa1 to regulate the PI3K-AKT signaling pathway. Further analysis using miRmap and IntaRNA tools revealed that LOC102547734 had a target binding site with miR-206-3p and miR-206-3p with Hsp90aa1 (Fig. 8).

Our study has several limitations. The small number of participants selected from a geographically restricted area constrains extrapolation of the results, pointing to the need for further studies with larger sample sizes. Moreover, the predominant reliance on bioinformatics analyses in the current literature pertaining to neurological damage associated with HS suggests the necessity for additional scrutiny of the upstream molecular components. Subsequent research should endeavor to construct ceRNA networks, substantiating the identified mechanisms through both *in vitro* cellular and *in vivo* animal experiments.

## Conclusions

In conclusion, our study presented evidence based on the analysis of differential mRNA expression in HS-induced neurological damage, suggesting the potential utility of the HS protein Hsp90aa1 as a prognostic marker for heat

stroke. (1) The observed downregulation of Hsp90AA1 may signify an unfavorable prognosis for nerve injury during the early stages of heat stroke. (2) Our findings led to the identification of a central lncRNA-miRNA-mRNA regulatory network, highlighting the putative significance of LOC102547734-MIR-206-3p-HSP90aa1 as a critical ceRNA network in preventing HS-induced nerve damage. (3) We expect that by introducing these novel insights, our study will contribute to the theoretical framework for understanding the pathogenesis of neurological damage in heat stroke and foster the development of targeted drug therapies to mitigate HS-induced effects.

**Acknowledgements** The authors would like to express their deepest appreciation to John Francis Bowyer and his team for publicly sharing the GSE64778 data.

**Author Contribution** Conception and design of the research: LW. Acquisition of data: YI-S, XC, QP, ZY-C, and HY-J. Analysis and interpretation of data: LW. Statistical analysis: HC. Obtaining financing: LW. Writing of the manuscript: LW. Critical revision of the manuscript for intellectual content: BF-Z and YZ. All authors read and approved the final draft.

**Funding** This work was supported by grants from the Medical Research Project of Jiangsu Provincial Health and Health Commission (Z2022067); the “Top Six Types of Talents” Financial Assistance of Jiangsu Province Grant (WSW-199); the “Scientific Research Innovation Team Project” of Kangda College of Nanjing Medical University (KD2022KYCXTD006); and the Scientific Research Foundation of Nantong Health and Health Commission (MB2021018, MB2021026).

**Data Availability** Data will be made available on request.

## Declarations

**Ethics Approval and Consent to Participate** This study was approved by the Second Hospital of Nantong University, Jiangsu Province, China (approval number 2021KT007). The study complied with the principles of the Declaration of Helsinki.

**Consent for Publication** Not applicable.

**Competing Interests** The authors declare no competing interests.

## References

1. Zhang ZT, Gu XL, Zhao X, He X, Shi HW, Zhang K, Zhang YM, Su YN et al (2021) NLRP3 ablation enhances tolerance in heat stroke pathology by inhibiting IL-1 $\beta$ -mediated neuroinflammation. *J Neuroinflammation* 18(1):128. <https://doi.org/10.1186/s12974-021-02179-y>
2. Périard JD, DeGroot D, Jay O (2022) Exertional heat stroke in sport and the military: epidemiology and mitigation. *Exp Physiol* 107(10):1111–1121. <https://doi.org/10.1113/EP090686>
3. He S, Li R, Peng Y, Wang Z, Huang J, Meng H, Min J, Wang F et al (2022) ACSL4 contributes to ferroptosis-mediated rhabdomyolysis in exertional heat stroke. *J Cachexia Sarcopenia Muscle* 13(3):1717–1730. <https://doi.org/10.1002/jcsm.12953>
4. Shimazaki T, Anzai D, Watanabe K, Nakajima A, Fukuda M, Ata S (2022) Heat stroke prevention in hot specific occupational


- environment enhanced by supervised machine learning with personalized vital signs. *Sensors (Basel)* 22(1):395. <https://doi.org/10.3390/s22010395>
5. Wei D, Gu T, Yi C, Tang Y, Liu F (2022) A nomogram for predicting patients with severe heatstroke. *Shock* 58(2):95–102. <https://doi.org/10.1097/SHK.0000000000001962>
  6. Maiti S, Picard D (2022) Cytosolic Hsp90 Isoform-specific functions and clinical significance. *Biomolecules* 12(9):1166. <https://doi.org/10.3390/biom12091166>
  7. Peng C, Zhao F, Li H, Li L, Yang Y, Liu F (2022) HSP90 mediates the connection of multiple programmed cell death in diseases. *Cell Death Dis* 13(11):929. <https://doi.org/10.1038/s41419-022-05373-9>
  8. Wang RY, Noddings CM, Kirschke E, Myasnikov AG, Johnson JL, Agard DA (2022) Structure of Hsp90-Hsp70-Hop-GR reveals the Hsp90 client-loading mechanism. *Nature* 601(7893):460–464. <https://doi.org/10.1038/s41586-021-04252-1>
  9. Somogyvári M, Khatatneh S, Söti C (2022) Hsp90: from cellular to organismal proteostasis. *Cells* 11(16):2479. <https://doi.org/10.3390/cells11162479>
  10. Noddings CM, Wang RY, Johnson JL, Agard DA (2022) Structure of Hsp90-p23-GR reveals the Hsp90 client-remodelling mechanism. *Nature* 601(7893):465–469. <https://doi.org/10.1038/s41586-021-04236-1>
  11. Rutledge BS, Choy WY, Duennwald ML (2022) Folding or holding?-Hsp70 and Hsp90 chaperoning of misfolded proteins in neurodegenerative disease. *J Biol Chem* 298(5):101905. <https://doi.org/10.1016/j.jbc.2022.101905>
  12. Roe SM, Török Z, McGown A, Horváth I, Spencer J, Pázmány T, Vigh L, Prodromou C (2023) The crystal structure of the Hsp90-LA1011 complex and the mechanism by which LA1011 may improve the prognosis of Alzheimer's disease. *Biomolecules* 13(7):1051. <https://doi.org/10.3390/biom13071051>
  13. Hu JM, Hsu CH, Lin YC, Kung CW, Chen SY, Lin WT, Cheng PY, Shen HH et al (2021) Ethyl pyruvate ameliorates heat stroke-induced multiple organ dysfunction and inflammatory responses by induction of stress proteins and activation of autophagy in rats. *Int J Hyperthermia* 38(1):862–874. <https://doi.org/10.1080/02656736.2021.1931479>
  14. Camacho L, Silva CS, Hanig JP, Schleimer RP, George NI, Bowyer JF (2019) Identification of whole blood mRNA and microRNA biomarkers of tissue damage and immune function resulting from amphetamine exposure or heat stroke in adult male rats. *PLoS One* 14(2):e0210273. <https://doi.org/10.1371/journal.pone.0210273>
  15. Li G, Guo Q, Liu Y, Li Y, Pan X (2018) Projected temperature-related years of life lost from stroke due to global warming in a temperate climate city, Asia: disease burden caused by future climate change. *Stroke* 49(4):828–834. <https://doi.org/10.1161/STROKEAHA.117.020042>
  16. Ni XX, Wang CL, Guo YQ, Liu ZF (2022) Analysis of clinical symptoms of Guillain-Barré syndrome induced by heat stroke: three case reports and literature review. *Front Neurol* 17(13):910596. <https://doi.org/10.3389/fneur.2022.910596>
  17. Yuan R, Wang L, Deng ZH, Yang MM, Zhao Y, Hu J, Zhang Y, Li Y et al (2023) Protective effects of mesenchymal stem cells against central nervous system injury in heat stroke. *Curr Stem Cell Res Ther* 18(3):401–409. <https://doi.org/10.2174/1574888X17666220511144254>
  18. DeGroot DW, O'Connor FG, Roberts WO (2022) Exertional heat stroke: an evidence based approach to clinical assessment and management. *Exp Physiol* 107(10):1172–1183. <https://doi.org/10.1113/EP090488>
  19. Infantino R, Schiano C, Luongo L, Paino S, Mansueto G, Boccella S, Guida F, Ricciardi F et al (2022) MED1/BDNF/TrkB pathway is involved in thalamic hemorrhage-induced pain and depression by regulating microglia. *Neurobiol Dis* 164:105611. <https://doi.org/10.1016/j.nbd.2022.105611>
  20. Long HZ, Cheng Y, Zhou ZW, Luo HY, Wen DD, Gao LC (2021) PI3K/AKT signal pathway: a target of natural products in the prevention and treatment of Alzheimer's disease and Parkinson's disease. *Front Pharmacol* 15(12):648636. <https://doi.org/10.3389/fphar.2021.648636>
  21. Jin T, Zhang Y, Botchway BOA, Zhang J, Fan R, Zhang Y, Liu X (2022) Curcumin can improve Parkinson's disease via activating BDNF/PI3k/Akt signaling pathways. *Food Chem Toxicol* 164:113091. <https://doi.org/10.1016/j.fct.2022.113091>
  22. Hua H, Zhang W, Li J, Li J, Liu C, Guo Y, Cheng Y, Pi F et al (2021) Neuroprotection against cerebral ischemia/reperfusion by dietary phytochemical extracts from Tibetan turnip (*Brassica rapa* L.). *J Ethnopharmacol* 30(265):113410. <https://doi.org/10.1016/j.jep.2020.113410>
  23. Wang L, Shen YM, Qian C et al (2021) Effect of circhp3 on polarization of microglial cells in nerve injury caused by heat radiation. *Chin J Emerg Med* 30(4):452–458. <https://doi.org/10.21203/rs.3.rs-112893/v1>
  24. Liu Z, Chen J, Hu L, Li M, Liang M, Chen J, Lin H, Zeng Z et al (2020) Expression profiles of genes associated with inflammatory responses and oxidative stress in lung after heat stroke. *Biosci Rep* 40(6):BSR20192048. <https://doi.org/10.1042/BSR20192048>
  25. Xing C, Liu XF, Zhang CF, Yang L (2021) Hsp90-associated DNA replication checkpoint protein and proteasome-subunit components are involved in the age-related macular degeneration. *Chin Med J (Engl)* 134(19):2322–2332. <https://doi.org/10.1097/CM9.0000000000001773>
  26. Wang L, Zhao H, Zhang L, Luo H, Chen Q, Zuo X (2020) HSP90AA1, ADRB2, TBL1XR1 and HSPB1 are chronic obstructive pulmonary disease-related genes that facilitate squamous cell lung cancer progression. *Oncol Lett* 19(3):2115–2122. <https://doi.org/10.3892/ol.2020.11318>
  27. Mohanapriya R, Akshaya RL, Selvamurugan N (2022) A regulatory role of circRNA-miRNA-mRNA network in osteoblast differentiation. *Biochimie* 193:137–147. <https://doi.org/10.1016/j.biochi.2021.11.001>
  28. Sadeghi M, Bahrami A, Hasankhani A, Kioumars H, Nouralizadeh R, Abdulkareem SA, Ghafouri F, Barkema HW (2022) lncRNA-miRNA-mRNA ceRNA network involved in sheep prolificacy: an integrated approach. *Genes (Basel)* 13(8):1295. <https://doi.org/10.3390/genes13081295>
  29. Chen L, Wei K, Li J, Li Y, Cao H, Zheng Z (2022) Integrated analysis of lncRNA-mediated ceRNA network in calcific aortic valve disease. *Cells* 11(14):2204. <https://doi.org/10.3390/cells11142204>
  30. Zhu J, Chen Y, Ji J, Wang L, Xie G, Tang Z, Qu X, Liu Z et al (2022) Microglial exosomal miR-466i-5p induces brain injury via promoting hippocampal neuron apoptosis in heatstroke. *Front Immunol* 12(13):968520. <https://doi.org/10.3389/fimmu.2022.968520>
  31. Li Y, Wen Q, Chen H, Wu H, Liu B, Li H, Su L, Tong H (2021) Exosomes derived from heat stroke cases carry miRNAs associated with inflammation and coagulation cascade. *Front Immunol* 12(12):624753. <https://doi.org/10.3389/fimmu.2021.624753>
  32. Li P, Luo X, Luo Z, He GL, Shen TT, Yu XT, Wang ZZ, Tan YL et al (2022) Increased miR-155 in microglial exosomes following heat stress accelerates neuronal autophagy via their transfer into neurons. *Front Cell Neurosci* 11(16):865568. <https://doi.org/10.3389/fncel.2022.865568>
  33. Dosil SG, Lopez-Cobo S, Rodriguez-Galan A, Fernandez-Delgado I, Ramirez-Huesca M, Milan-Rois P, Castellanos M, Somoza A et al (2022) Natural killer (NK) cell-derived extracellular-vesicle shuttled microRNAs control T cell responses. *Elife* 29(11):e76319. <https://doi.org/10.7554/eLife.76319>

**Publisher's Note** Springer Nature remains neutral with regard to jurisdictional claims in published maps and institutional affiliations.

Springer Nature or its licensor (e.g. a society or other partner) holds exclusive rights to this article under a publishing agreement with the author(s) or other rightsholder(s); author self-archiving of the accepted manuscript version of this article is solely governed by the terms of such publishing agreement and applicable law.



## Authors and Affiliations

Lei Wang<sup>1</sup> · Yi-ming Shen<sup>1</sup> · Xin Chu<sup>1</sup> · Qiang Peng<sup>1</sup> · Zhi-yong Cao<sup>2</sup> · Hui Cao<sup>3</sup> · Han-yu Jia<sup>4</sup> · Bao-feng Zhu<sup>1</sup> · Yi Zhang<sup>4,5</sup> 

✉ Bao-feng Zhu  
bfzhunt1@163.com

✉ Yi Zhang  
zhangyi9285@126.com

<sup>1</sup> Department of Emergency Center, Second Affiliated Hospital of Nantong University, No. 6 North, Child Lane Road, Nantong, China

<sup>2</sup> Department of Neurology, Second Affiliated Hospital of Nantong University, No. 6, North Child Lane Road, Nantong, China

<sup>3</sup> Department of Rehabilitation, Second Affiliated Hospital of Nantong University, No. 6, North Child Lane Road, Nantong, China

<sup>4</sup> Research and Education Sector, Second Affiliated Hospital of Nantong University, No. 6, North Child Lane Road, Nantong, China

<sup>5</sup> Department of Neurosurgery, Second Affiliated Hospital of Nantong University, No. 6, North Child Lane Road, Nantong, China